Molecular Crystals and Liquid Crystals

Publication details, including instructions for authors and subscription information:
http://www.tandfonline.com/loi/gmcl20

Comparison of Microwave Measurements and Theoretical Calculations of Dielectric Birefringence for a Liquid Crystal Loaded CPW-FE Phase Shifter

Yozo Utsumi [a], Nguyen Thanh Bach [a], Toshihisa Kamei [a], Ryotaro Ozaki [a] & Hiroshi Moritake [a]

[a] Department of Communications Engineering, National Defense Academy, Kanagawa, Japan

Version of record first published: 05 Oct 2009

To cite this article: Yozo Utsumi, Nguyen Thanh Bach, Toshihisa Kamei, Ryotaro Ozaki & Hiroshi Moritake (2009): Comparison of Microwave Measurements and Theoretical Calculations of Dielectric Birefringence for a Liquid Crystal Loaded CPW-FE Phase Shifter, Molecular Crystals and Liquid Crystals, 510:1, 197/[1331]-213/[1347]

To link to this article: http://dx.doi.org/10.1080/15421400903112085

Mol. Cryst. Liq. Cryst., Vol. 510, pp. 197/[1331]–213/[1347], 2009

ISSN: 1542-1406 print/1563-5287 online
DOI: 10.1080/15421400903112085

Comparison of Microwave Measurements and Theoretical Calculations of Dielectric Birefringence for a Liquid Crystal Loaded CPW-FE Phase Shifter

Yozo Utsumi, Nguyen Thanh Bach, Toshihisa Kamei, Ryotaro Ozaki, and Hiroshi Moritake
Department of Communications Engineering, National Defense Academy, Kanagawa, Japan

The effective permittivity and the variable phase shift of a microwave phase shifter using a liquid crystal loaded coplanar waveguide with floating electrode (CPW-FE), and the dielectric birefringence ($\Delta\varepsilon$) of the liquid crystal layer in a liquid crystal microwave phase shifter are calculated, taking into account molecular orientations in a liquid crystal layer. The effective permittivity and the dielectric birefringence are determined from the liquid crystal molecular orientations and CPW-FE high-frequency electric field. Using liquid crystal continuum theory, we obtain a liquid crystal molecular orientation controlled by a bias voltage. Calculations of the dependence of the variable phase shift on the bias voltage and the dielectric birefringence qualitatively agree with measurements. Furthermore, the calculations confirm the mechanism of the change in permittivity.

Keywords: CPW-FE; dielectric birefringence; molecular orientation; nematic liquid crystal; phase shift

1. INTRODUCTION

As a reflection of user needs in an age when multi-media, multi-channel services are being delivered to users through various transmission paths, there is a need to develop variable-function devices for the microwave and millimeter wave bands. Liquid crystals are receiving much attention as a material for achieving this, due to the ability to electrically control their permittivity.

Address correspondence to Yozo Utsumi, Department of Communications Engineering, National Defense Academy, Hashirimizu 1-10-20, Yokosuka-shi, Kanagawa 239-8686, Japan. E-mail: yutsumi@nda.ac.jp

Currently, microstrip line (MSL) structures are commonly used in development of liquid crystal devices for the microwave band (variable delay lines and variable phase shifters), but speeding up the response time has been a challenge [1]. With MSL structures, the orientation of the liquid crystal molecules is controlled by the presence or absence of an applied voltage, so it is possible to improve the response time when applying the voltage by increasing the applied voltage. However, when the voltage is removed, the response is determined by the relaxing of molecule positions, and this time cannot be reduced by increasing voltage. The response time after removing the voltage is also dependent on the thickness of the liquid-crystal layer, so MSL devices must be designed with a thinner liquid-crystal layer to achieve faster response times. However, with MSL structures, as with liquid-crystal displays, if the liquid-crystal layer is made very thin, insertion noise increases dramatically. This makes it difficult to create a fast device with low insertion loss. To resolve this difficulty, we have proposed a liquid crystal device with a "coplanar waveguide with floating electrode" (CPW-FE) structure [2,3]. With the CPW-FE structure, the orientation of the liquid crystal molecules is controlled by applying driving voltages in the vertical and horizontal directions to vary the permittivity felt by the dominant mode of the radio-frequency electric field in the CPW. With this structure, the liquid crystal can be placed in two different orientations controlled by applying a voltage, so unlike the MSL structure, it is easier to speed up the response time. However, with the CPW-FE structure, the orientation within the liquid crystal layer is more complex, making it difficult to derive the theoretical effective permittivity of the CPW-FE, and detailed liquid crystal orientation distributions must be computed. In this research, we compute distributions of liquid crystal molecules within the CPW-FE structure based on liquid crystal continuum theory, and attempt to derive the dielectric birefringence ($\Delta\varepsilon$), which is the change in effective permittivity of the CPW-FE. We manufactured four devices with this structure and differing parameters, measured how the amount of phase change varied with applied voltage, and compared results of measuring the phase change and dielectric birefringence ($\Delta\varepsilon$) of the liquid crystal layer with the calculated values.

2. STRUCTURE AND MANUFACTURING OF THE LIQUID CRYSTAL LOADED CPW-FE VARIABLE PHASE SHIFTER

External and cross-sectional views of the liquid crystal loaded CPW-FE variable phase shifter are shown in Figure 1. The CPW is manufactured on a microwave substrate with a 345 μm thick dielectric

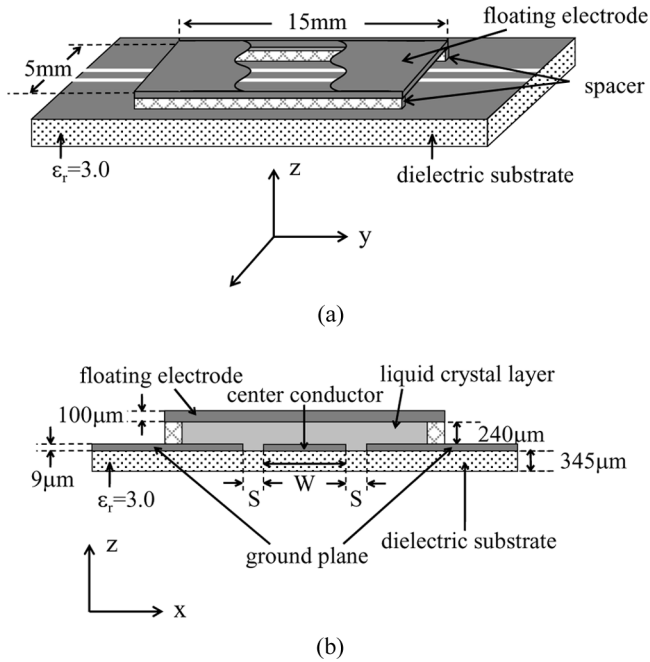

FIGURE 1 Structure crystal loaded variable phase shifter using coplanar waveguide with floating electrode. (a) External view, and (b) Cross-sectional view.

layer of relative permittivity $\varepsilon_r = 3.0$ and 9 μm metallic layer of copper. In the figure, W is the width of the center conductor, and S is the gap between the center conductor and the ground plane. The upper part of the CPW consists of a $5\,\text{mm} \times 15\,\text{mm} \times 100\,\mu\text{m}$ floating electrode positioned parallel to the CPW substrate using 240 μm-thick spacers. After the floating electrode is positioned, the space between the electrode and the CPW is filled with a nematic liquid crystal (BL006, Merck). Note that no particular orienting process (no rubbing process) is performed between the floating electrode and CPW substrate surface.

In this research, we were investigating the effect of the widths, W, of the central conductor and S, of the gap between the central conductor and the ground plane, on the amount of phase-change in the CPW-FE. Accordingly, we manufactured three devices with $S = 70\,\mu\text{m}$ and $W = 50$, 200, and 300 μm respectively, and one with $S = 140\,\mu\text{m}$, and $W = 50\,\mu\text{m}$. The effective path length of the CPW-FE is 15 mm. The dependence of phase change on applied voltage in the 10–30 GHz band for the four manufactured devices was measured using a network analyzer (37369C, Anritsu).

As shown in Figure 2, a liquid crystal driving bias voltage was applied between the floating electrode and CPW central conductor and the ground plane in one case, and between the CPW central conductor and the ground plane in the other. By switching between these two, two device states, and two phase-change amounts, are achieved for microwaves transmitted by the CPW-FE.

Figure 2(a) shows the case with the bias voltage applied between the floating electrode and center conductor and ground plane, and

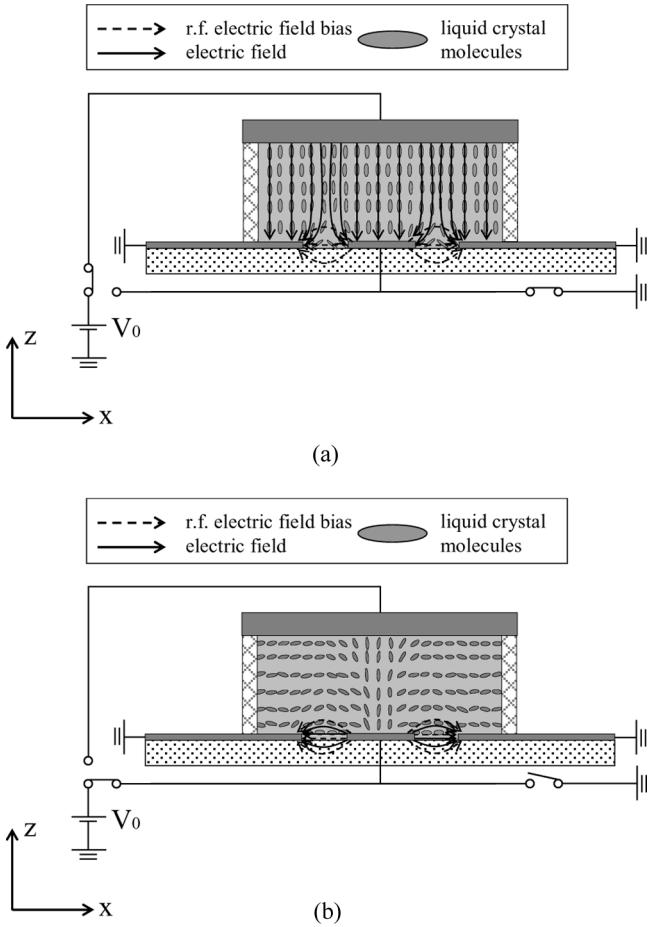

FIGURE 2 Liquid crystal molecular orientation in a CPW-FE. (a) Liquid crystal molecular orientation when a voltage is applied to the floating electrode. (b) Liquid crystal molecular orientation when a voltage is applied to the center conductor.

Figure 2(b) shows the case with it applied between the CPW center conductor and the ground plane. Figure 2 also shows a representation of the orientation of liquid crystal molecules. In Figure 2(a), the liquid crystal driving bias electrical field is generated between the floating electrode and the CPW center conductor and ground plane, so the long axis of the liquid crystal molecules is oriented in the z direction. In this case, the radio-frequency electric field in the area of the gap between the center conductor and the ground plane is mostly perpendicular to the liquid crystal molecules, so it feels the permittivity of the short axis of the molecules ($\varepsilon_{\perp}$). Conversely, in Figure 2(b), the liquid crystal bias field is mostly the same as the CPW radio-frequency electric field, so in the gap area, the radio-frequency electric field feels the permittivity of the long axis of the molecules ($\varepsilon_{\parallel}$). In other words, by changing the direction of the applied bias voltage, the orientation of the liquid crystal molecules in the gap where the radio-frequency electric field is high in the CPW can be changed to either perpendicular or parallel to the CPW-FE radio-frequency electric field direction. For our experiments, we applied these two bias voltages by driving the device with a control circuit having two linked external relay switches.

3. COMPUTATION OF LIQUID CRYSTAL ORIENTATION DISTRIBUTION AND THE EFFECTIVE PERMITTIVITY OF THE CPW-FE

3.1. Computation of Orientation Distribution Based on Liquid Crystal Continuum Theory

If the energy density of the orientation field is f, then the fundamental equation of continuum theory when an electrical field E is applied is as in Eq. (1) [4].

$$\mathrm{f} = \frac{1}{2}\mathrm{K}_1(\nabla \cdot \mathbf{n})^2 + \frac{1}{2}\mathrm{K}_2(\mathbf{n} \cdot \nabla \times \mathbf{n})^2 + \frac{1}{2}\mathrm{K}_3(\mathbf{n} \times \nabla \times \mathbf{n})^2 - \frac{1}{2}\varepsilon_0 \Delta\varepsilon_{lf}(\mathrm{E} \cdot \mathbf{n})^2 \tag{1}$$

Here, ε_0 is the permittivity of free space, $\Delta\varepsilon_{\mathrm{lf}}$ is the low-frequency dielectric birefringence of the liquid crystal molecules, **n** is the liquid crystal molecule director (a unit vector in the direction of the long axis of the liquid crystal molecules), and K_1, K_2, and K_3 are the elastic constants for splay, twist and bend, respectively.

Here, if the angle between the director and the x-axis is φ, so that $(\mathrm{n_x}, \mathrm{n_z}) = (\cos\varphi, \sin\varphi)$, then when electric field $\mathrm{E} = (\mathrm{E_x}, \mathrm{E_z})$ is

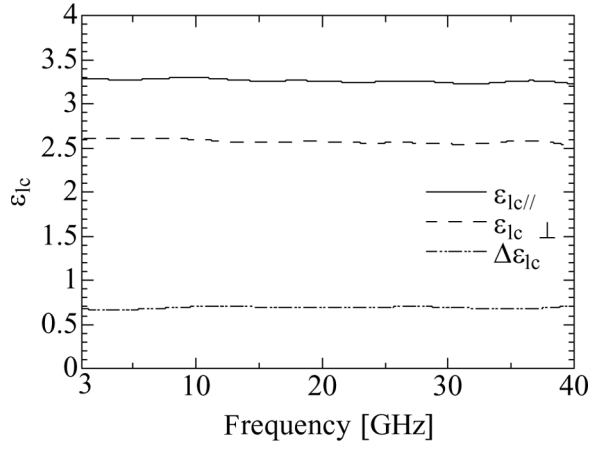

FIGURE 3 Permittivity of liquid crystal material (BL006) by cutback method.

applied, the energy density, f, of a liquid-crystal molecule rotating in the x–z plane is given by Eq. (2). Note that for Figure 2 and Eq. (1), no rubbing process was used, so the twist deformation shown in Figure 3(b) is not considered, and K_2 is set to zero. In other words, our analysis considers the 2-dimensional problem in the x–z plane.

$$\begin{aligned} f = {} & \frac{1}{2}(K_1 \sin^2\varphi + K_3 \cos^2\varphi)\left(\frac{d\varphi}{dx}\right)^2 \\ & + \frac{1}{2}(K_1 \cos^2\varphi + K_3 \sin^2\varphi)\left(\frac{d\varphi}{dz}\right)^2 \\ & + (K_3 - K_1)\sin\varphi\cos\varphi\frac{d\varphi}{dx}\frac{d\varphi}{dz} - \frac{1}{2}\varepsilon_0\Delta\varepsilon_{lf}(E_x\cos\varphi + E_z\sin\varphi)^2 \end{aligned} \tag{2}$$

The equations of motion for the director, considering conservation of momentum and energy, are given in Eq. (3) [4].

$$\gamma\frac{\partial\varphi}{\partial t} = -\frac{\partial f}{\partial\varphi} + \frac{d}{dx}\left\{\frac{\partial f}{\partial(d\varphi/dx)}\right\} + \frac{d}{dz}\left\{\frac{\partial f}{\partial(d\varphi/dz)}\right\} \tag{3}$$

Here, γ is the rotational viscosity. Substituting (2) into (3) and solving for φ gives the liquid crystal molecular orientation distribution. For this paper, we discretize (3) and solve it numerically to compute the orientation distribution of the liquid crystal molecules in the liquid crystal layer of the CPW-FE.

3.2. Computing the Effective Permittivity of the CPW-FE

In order to compute the effective permittivity of the liquid crystal loaded CPW-FE, the electric field driving the liquid crystal, the liquid crystal molecular orientation distribution, and the CPW-FE radio-frequency electric field must all be computed. We will first discuss the computation of the liquid crystal bias electric field and the liquid crystal orientation distribution.

As discussed in the previous section, the applied electrical field is required in order to compute the orientation distribution of the liquid crystal molecules. For this research, we computed the liquid crystal bias electric field by discretizing the Laplace equation and solving iteratively. We used a 1 μm discretization mesh, and applied Neumann boundary conditions ($dV/dx = 0$, where V is the applied voltage) at the upper left and right boundaries of the ground plane. Note that we have computed the electrical field generated between the electrodes assuming the permittivity of the liquid crystal layer to be constant, but actually, as the orientation of the liquid crystal molecules changes, the permittivity of the liquid crystal layer also changes gradually. A computation of the electrical field taking changes in the permittivity distribution into account would be extremely complex, so for this research we assume the permittivity felt by the liquid crystal bias electric field is approximately constant.

After computing the bias electric field, it is substituted into Eq. (3) to get the liquid crystal molecular orientation distribution. The liquid crystal properties used in the computation were $\gamma = 71\,\mathrm{mPa \cdot s}$, $K_1 = 17.9\,\mathrm{pN}$, $K_3 = 33.5\,\mathrm{pN}$, $\varepsilon_0 = 8.854 \times 10^{-12}\,\mathrm{F/m}$, and $\Delta\varepsilon_{lf} = 17.3$. The discretization mesh interval used was 1 μm as with the bias electric field computation. For boundaries in the x direction on the floating electrode, center conductor and the ground plane, boundary conditions were set anchoring the liquid crystal molecules parallel to the surface strongly, with $\varphi = 0$. Neumann boundary conditions were set for boundaries on the ground plane in the z direction.

Conversely, if the relative permittivities of the dielectric substrate and the liquid crystal material used in the liquid crystal layer are ε_r, and ε_{lc} respectively, the effective permittivity, felt by the radio-frequency field, E_h, in the liquid crystal loaded CPW-FE phase shifter shown in Figure 1, is given in Eq. (4) [5],

$$\varepsilon_{eff} = \frac{\varepsilon_r \int_{S1} \mathbf{E}_h^2 d\mathbf{s} + \int_{S2} \varepsilon_{lc} \mathbf{E}_h^2 d\mathbf{s}}{\int_{S1+S2} \mathbf{E}_h^2 d\mathbf{s}} \tag{4}$$

where S1 and S2 express the CPW-FE dielectric and liquid crystal regions respectively.

The radio-frequency electric field, $E_h(x, z)$, in the CPW-FE and the liquid-crystal molecule director, $\mathbf{n}(x, z)$ distributions were calculated, and then the relative permittivity, $\varepsilon_{lc}(x, z)$, at each grid point in the space was calculated using Eq. (5) [6].

$$\frac{1}{2}\varepsilon_{lc}(x,z)E_h^2(x,z) = \frac{1}{2}\varepsilon_{lc\perp}(x,z)E_h^2(x,z) + \frac{1}{2}\Delta\varepsilon_{lc}\{E_h(x,z)\cdot\mathbf{n}(x,z)\}^2 \quad (5)$$

Actually, $\varepsilon_{lc\perp}$is the relative permittivity of the liquid crystal material felt by the radio-frequency electric field when the long axis of the liquid crystal molecules is perpendicular to the radio-frequency electric field, $\varepsilon_{lc\|}$ is the relative permittivity when the long axis is parallel, and $\Delta\varepsilon_{lc}$ is the dielectric birefringence of the liquid crystal material, given by Eq. (6).

$$\Delta\varepsilon_{lc} = \varepsilon_{lc//} - \varepsilon_{lc\perp} \quad (6)$$

The liquid crystal material characteristic values, $\varepsilon_{lc\perp}$ and $\varepsilon_{lc\|}$, were derived experimentally using the cutback method in Ref. [7] and are shown in Figure 3. As can be seen from the figure, the relative permittivities, $\varepsilon_{lc\perp}(2.57)$ and $\varepsilon_{lc\|}(3.26)$ as well as the dielectric birefringence, $\Delta\varepsilon_{lc}$ (0.69), are mostly constant through the 3 to 40 GHz range. These values can be substituted into Eq. (4) and (5) to determine ε_{eff}.

In the computations for (4) and (5), ε_{lc} has a spatial distribution, so the radio-frequency electric field strength was used as a weighting factor. Regions where the radio-frequency electric field is strong have a stronger dielectric effect. We approximate the radio-frequency electric field in the CPW-FE as a TEM wave, and compute it using a discretized Laplace method, as we did with the liquid crystal bias electric field. Also as with the liquid crystal bias electric field, we do not consider changes in permittivity due to changes in orientation of the liquid crystal molecules.

4. COMPARISON OF THE MEASURED AND COMPUTED PHASE-SHIFT RESULTS FOR THE LIQUID CRYSTAL LOADED CPW-FE PHASE SHIFTER

Figure 4 shows the computed results for the liquid crystal bias electric field when a voltage is applied to the floating electrode and the center conductor. Figure 4(a) shows the electric field distribution when the

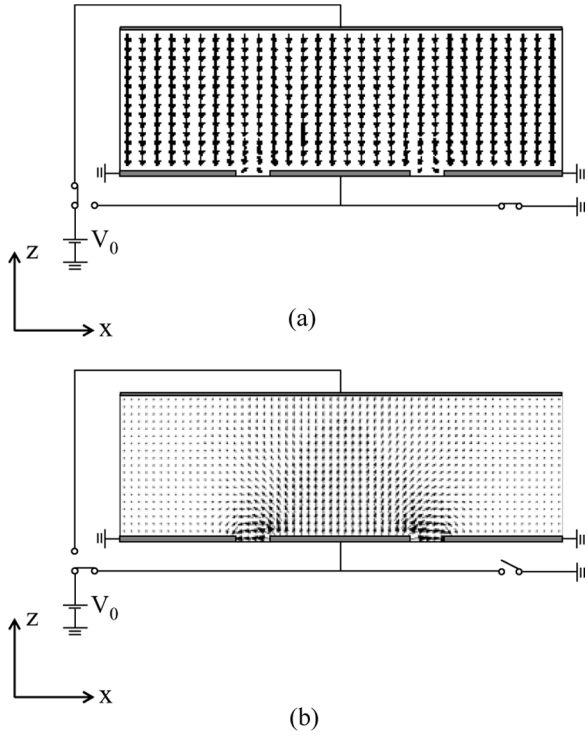

FIGURE 4 Bias electric field distribution for liquid crystal orientation control. (a) When a 100 V is applied to the floating electrode. (b) When a 100 V is applied to the center conductor.

floating electrode has a potential of 100 V and the center conductor and ground plane have 0 V. When the potential is applied to the floating electrode, an electric field in the z-axis direction is generated through the whole liquid crystal layer, and wraps around the gap between the center conductor and the ground plane. Conversely, when the center conductor has a potential of 100 V and the floating electrode and ground plane are at 0 V, the electric field distribution is as shown in Figure 4(b). When a voltage is applied to the center conductor, an electric field forms toward the floating electrode, but it is concentrated near the gap between center conductor and ground plane, which is a shorter distance.

Next, the liquid crystal molecular orientation distribution is computed by substituting the liquid crystal bias electric field into Eq. (3). The orientation distribution when 100 V is applied to the floating electrode is shown in Figure 5. The lines in the figure

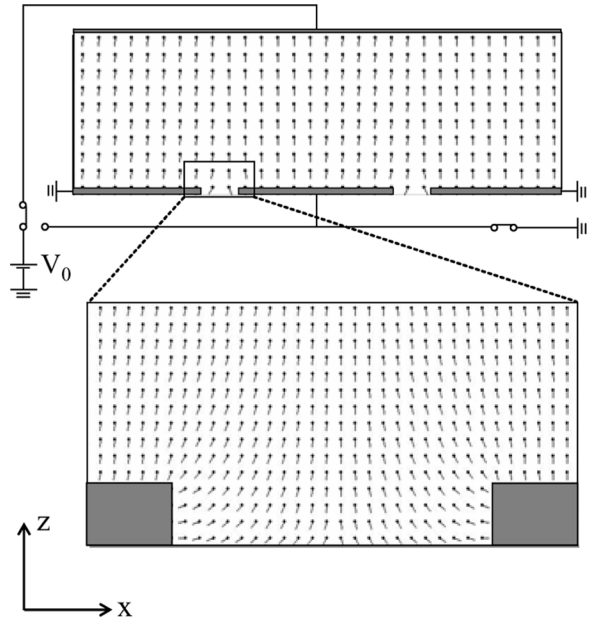

FIGURE 5 Molecular orientation when 100 V is applied to the floating electrode.

represent the liquid crystal director vectors, and it can be seen that the directors follow the direction of the electric field. In this case, most molecules in the liquid crystal layer are oriented parallel to the z-axis, but in the gap between the center conductor and the ground plane, the field wraps around, and the director vectors also wrap around, following the electric field. Conversely, the orientation distribution when 100 V is applied to the center conductor is shown in Figure 6. The liquid crystal molecules are oriented with the electric field shown in Figure 4(b), and in the gap between the center conductor and the ground plane, they are oriented in the direction of the x axis. These results confirm theoretically that the orientation of molecules in the liquid crystal layer can be changed between horizontal and vertical, as we had hoped.

The radio-frequency electric field and electric-field energy distributions for the CPW-FE are shown in Figure 7. As can be seen in Figure 7(a), there is an electric field from the center conductor to the floating electrode, but most of it is from the center conductor to the ground plane. Also, the electric-field energy distribution contributes to the effective permittivity of the CPW-FE phase shifter, so we have shown the electric-field energy distribution due to the radio-frequency

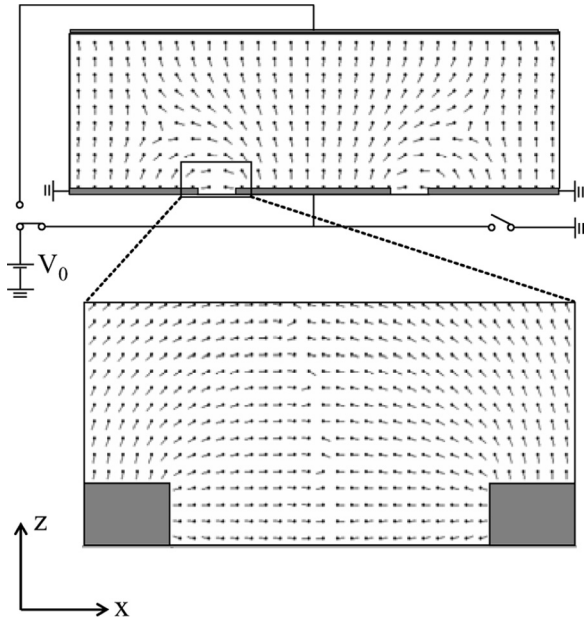

FIGURE 6 Molecular orientation when 100 V is applied to the center conductor.

electric field in Figure 7(b). As can be seen clearly in this figure, the electric field is concentrated in the gap between the center conductor and the ground plane, so changes in the orientation of the liquid crystal molecules in the area of this gap can be expected to have a significant effect on the permittivity of the CPW-FE phase shifter.

The liquid crystal molecular orientation distribution and the CPW-FE radio-frequency electric field distribution computed as above were substituted into Eqs. (4) and (5) to compute the effective permittivity, ε_{eff}, of the liquid crystal loaded CPW-FE phase shifter. The effective permittivity ε_{eff}, for the two bias states in Figure 2(a) and (b) are computed as $\varepsilon_{\text{effa}}$ and $\varepsilon_{\text{effb}}$. Phase shift of the CPW-FE phase shifter can be expressed as θ_{a} and θ_{b} corresponding to $\varepsilon_{\text{effa}}$ and $\varepsilon_{\text{effb}}$ respectively. Then the variable phase shift, $\Delta\theta_{\text{cal}}$, for path length, l, of 15 mm, and frequency f, of 20 GHz, can be computed as in Eq. (7),

$$\Delta\theta_{\text{cal}} = \theta_{\text{b}} - \theta_{\text{a}} = \frac{2\pi \text{fl}}{\text{c}} \left(\sqrt{\varepsilon_{\text{effb}}} - \sqrt{\varepsilon_{\text{effa}}}\right) \quad [\text{rad.}] \tag{7}$$

where c is light velocity.

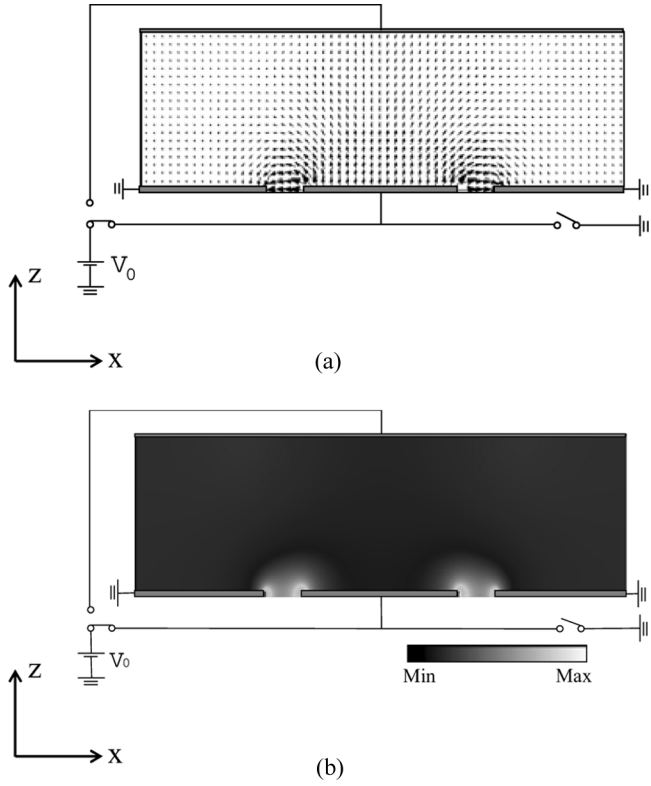

FIGURE 7 Radio- frequency electric field of CPW. (a) Electric field distribution. (b) Electric field energy distribution.

These results, compared with measured experimental phase shift values, $\Delta\theta_{exp}$, are shown in Figure 8 for the four combinations of center conductor width, W, and gap-width, S. To optimize the CPW-FE structure, we performed the calculations and measurements for four devices; three with $S = 70\,\mu m$ and $W = 50$, 200, and $300\,\mu m$ respectively, and one with $S = 140\,\mu m$ and $W = 50\,\mu m$.

In both measured and computed cases, as the bias voltage increased, the amount of phase shift, $\Delta\theta$, also increased. Furthermore, up to 20 V, $\Delta\theta$ increased rapidly, and above 20 V, it increased more gradually. This is because the orientation of the liquid crystal molecules is due to a balance between the electric field and elastic energy, so in the region up to 20 V the liquid crystal molecules are restricted elastically, and the director vectors gradually change to the electric field orientation. Then, above 20 V, most of the molecule

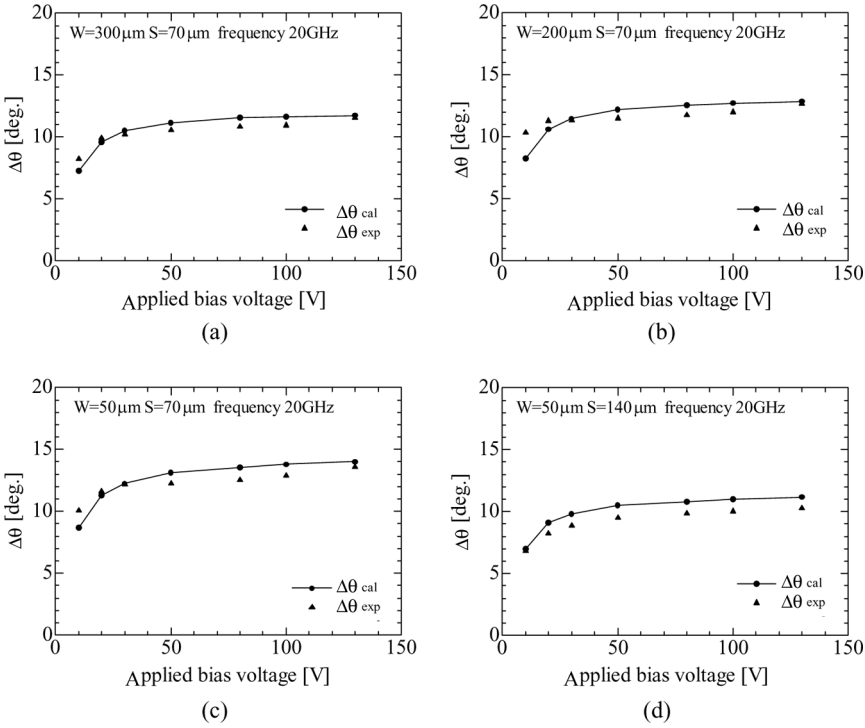

FIGURE 8 Variable phase shift of liquid crystal loaded CPW-FE phase shifter (l = 15 mm).

directors follow the electric field, and as the voltage continues to increase, only the molecules near the boundary, which are more strongly confined by the substrate, change slightly.

For both the measured and calculated values of $\Delta\theta$, in terms of the center conductor width, W, and gap-width S, values changed the most for (S, W) = (70 μm, 50 μm), followed by (70 μm, 200 μm), (70 μm, 300 μm), and (140 μm, 50 μm). This indicates, from both measured and calculated results, that the gap width is more significant than the center conductor width for achieving a large $\Delta\theta$. It also shows that the concentration of electric field around the gap between center conductor and ground plane is very important. By concentrating the electric field along the gap between center conductor and ground plane, where the liquid crystal molecules are most greatly changed as shown in Figures 5 and 6, the CPW-FE can use the change in permittivity of the liquid crystal more effectively. Conversely, as the width of the center conductor, W, is made smaller, $\Delta\theta$ gets larger.

This is because, as shown in Figure 7(a), the radio-frequency electric field goes from the center conductor to the ground plane, but liquid crystal molecules near the center of the center conductor are oriented along the z-axis regardless of whether voltage is applied to the floating electrode or the center conductor, as shown in Figures 5 and 6, and are not changed by changing the bias voltage direction. As a result, when the width of the center conductor is made smaller, the region where the orientation of liquid crystal is not changed (a dead region) becomes smaller, and this results in $\Delta\theta$ becoming larger.

Comparing the computed and measured results quantitatively, the computed values for $\Delta\theta$ were approximately 10% higher when the bias voltage was over 20 V, and the measured values were approximately 10% higher below 20 V, so the results do not agree perfectly. However, the change in the variable phase shift for the two corresponded very well qualitatively. A possible reason why the results did not match quantitatively is that in the experiments it was not possible to obtain the uniformity of orientation assumed in the computations. Another possible reason is that in the computations, we assumed that the anchoring of liquid crystal molecules in the gap area (S) was perfectly in the x direction ($\varphi = 0$) for both the conductor and the dielectric substrate, but in the experimental case it may have varied somewhat due to etching precision on the conductors. Also, when the bias voltage was below 20 V, since no rubbing processing was performed on the device, there would also be some liquid crystal molecules oriented along the y-axis on an actual device. These molecules would normally reflect the $\varepsilon_{lc\perp}$permittivity on the radio-frequency electric field in the bias state shown in Figure 2(a), imparting a large phase change. Possibilities also include the fact that changes in permittivity were not considered in the process of calculating the electric field distribution, and that the discretization mesh interval may have been too large. In the future we plan to improve the precision by computing the electric field distribution using a finer discretization mesh, and using a method which takes into account changes in permittivity.

5. COMPARISON OF COMPUTED AND MEASURED RESULTS FOR BIREFRINGENCE IN THE LIQUID CRYSTAL LAYER

To verify the amount of speed up, and conversely the amount of degradation in dielectric birefringence ($\Delta\varepsilon$) in the liquid crystal layer compared to the liquid crystal material itself, these values were both measured and computed for the liquid crystal loaded CPW-FE phase shifter, which was designed with the goal of speeding up response time. The effective permittivity of the liquid crystal layer, ε, can be

calculated by Eq. (8).

$$\varepsilon = \frac{\int_S \varepsilon_{lc} E_h^2 ds}{\int_S E_h^2 ds} \tag{8}$$

Here, S is the liquid crystal layer region. $\varepsilon_{lc}(x, z)$ can be computed using Eq. (5).

If ε for the two bias states in Figure 2 (a) and (b) are computed as ε_a and ε_b using Eqs. (5) and (8), then the dielectric birefringence, $\Delta\varepsilon_{cal}$, when changing between bias states in (a) and (b) can be computed as in Eq. (9).

$$\Delta\varepsilon_{cal} = \varepsilon_b - \varepsilon_a \tag{9}$$

On the other hand, a measured value for dielectric birefringence of the liquid crystal layer, $\Delta\varepsilon_{exp}$, can be calculated from measurements of variable phase shift when switching between the two bias states in Figure 2(a) and (b). Figure 9 shows the calculated and measured values, $\Delta\varepsilon_{cal}$ and $\Delta\varepsilon_{exp}$, for dielectric birefringence of the liquid crystal layer of the liquid crystal loaded CPW-FE phase shifter, for the case in Figure 8 that showed the highest phase shift (Fig. 8(c), $W = 50\,\mu m$, $S = 70\,\mu m$).

The dielectric birefringence of the liquid crystal layer showed almost the same tendency as the phase shift of the phase shifter, with computed and measured values agreeing within a 10% error margin.

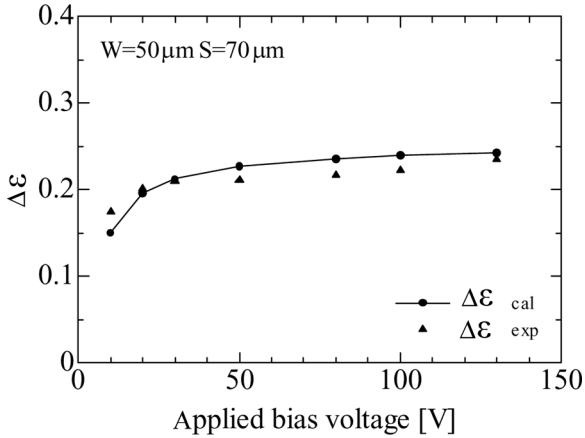

FIGURE 9 Dielectric birefringence of liquid crystal loaded CPW-FE phase shifter's liquid crystal layer.

The $\Delta\varepsilon_{lc}$ value for the liquid crystal material shown in Figure 3 is 0.69, so the $\Delta\varepsilon$ value of 0.25 for the CPW-FE structure liquid crystal layer in Figure 9 represents a degradation of approximately 36.2%.

6. CONCLUSIONS

By computing the molecular orientation distribution for the liquid crystal layer in a liquid crystal loaded CPW-FE phase shifter, we attempted to derive the theoretical effective permittivity, variable phase shift and dielectric birefringence in the microwave band for the liquid crystal layer. For four devices with different structural parameters, we measured the variable phase shift, and compared it with the computed results. The measured and computed results differed quantitatively by about 10%, but qualitative characteristics showed extremely good correspondence, and we were able to reproduce a liquid crystal loaded CPW-FE phase shifter with effective permittivity dependent on voltage. In addition to reproducing the experimental results, we were able to explain the effect of the widths of the center conductor and gap between center conductor and ground plane of the CPW-FE on the effective permittivity in terms of the liquid crystal molecular orientation distribution and the radio-frequency electric field in the liquid crystal loaded CPW-FE phase shifter, providing a logical explanation for the experimental results. We believe that the development of this computation method will be extremely important in optimizing the design of liquid crystal loaded CPW-FE phase shifters in the future. We plan to increase the precision of the computations by using a finer discretization mesh, and by analyzing microwave propagation in the liquid crystal, taking into consideration changes in permittivity.

REFERENCES

[1] Utsumi, Y., Kamei, T., Saito, K., & Naito, R. (Dec. 1994). Response time performance for microstrip-line type liquid crystal cevices. *The Transactions of the Institute of Electronics, Information and Communication Engineers (C)*, *J87-C*(12), 1086–1096.

[2] Utsumi, Y., Kamei, T., & Maeda, T. (Jun. 2007). Liquid crystal loaded high-speed microwave phase shifter using a coplanar path with floating electrode. *The Transactions of the Institute of Electronics, Information and Communication Engineers (C)*, *J90-C*(6), 483–490.

[3] Utsumi, Y. (Mar. 2007). Dielectric and response-time characteristics of a microwave liquid crystal device. *The Transactions of the Institute of Electronics, Information and Communication Engineers (C)*, *J90-C*(3), 197–207.

[4] de Gennes, P. G. & Prost, J. (1993). *The Physics of Liquid Crystal*, Oxford University Press.

[5] Onishi, K. (2001). *Lectures in Practical Microwave Technology – Theory and Practice – Vol. 1*, Nikkan Kogyo Shimbun Co. Inc., 122.
[6] Orihara, H. (2004). *Liquid Crystal Physics*, Uchida Rokakuho, 38.
[7] Kamei, T., Utsumi, Y., Moritake, H., Toda, K., & Suzuki, H. (Dec. 2002). Dielectric properties measurements of nematic liquid crystal at 10 kHz–40 GHz and the application for variable delay line. *The Transactions of the Institute of Electronics, Information and Communication Engineers (C)*, *J85-C*(12), 1149–1158.